

Lean or Ultra-Lean Stretched Propane/Air Counterflow Flames

Zhongxian Cheng*, Joseph A. Wehrmeyer, and Robert W. Pitz
Mechanical Engineering Department, Vanderbilt University
Box 1592 Station B, Nashville, TN 37235

Stretched laminar flame structures for a wide range of propane/air mixtures versus hot products are investigated by laser-based diagnostics and numerical simulation. The effect of stretch rate and equivalence ratio on four groups of flame structures is studied in detail by Raman scattering measurement and numerical calculations of the major species concentration and temperature profiles. The equivalence ratio varies from near stoichiometric ($\phi=0.86$) to sub-lean limit ($\phi=0.44$) values and the stretch rate varies from 90 s^{-1} to near extinction. For most of these lean mixtures, hot products are needed to maintain the flame. The significant feature of these flames is the relatively low flame temperature ($1200\text{ K} \sim 1800\text{ K}$). For this temperature range, the propane/air flame structure is sensitive to the specific chemical kinetic mechanism. Two types of flame structures (lean self-propagating flame and lean diffusion-controlled flame) are obtained based on the combined effect of stretch and equivalence ratio. Three different mechanisms, the M5 mechanism, the Optimized mechanism and the Williams mechanism, are chosen for the numerical simulations. None of the propane chemical mechanisms give good agreement with the data over the entire range of flame conditions.

INTRODUCTION

Lean combustion is currently under investigation due to its potential advantages in limiting thermal NO_x emissions and in reducing fuel consumption. It has been used in lean direct injected gas turbines and direct injection spark ignition (DISI) engines. But a critical problem is that lean direct-injected combustion tends to produce unburned hydrocarbon pollutants. This is because in lean direct injection combustion, the fuel/air mixing is inhomogeneous. The mixture in some regions is so lean that it doesn't burn. But this ultra lean mixture may still react if hot products interact with it. That is, under certain conditions, the lean mixture region can burn and thus reduce the potential pollutants. The interaction of lean mixtures with hot products needed to maintain the lean region burning is the focus of this work.

Considering the various conditions that exist simultaneously in inhomogeneous fuel/air reaction, a set of C₃H₈/air flames with a wide range of equivalence ratios and stretch rates impinging upon downstream hot products are studied experimentally and numerically. The opposed jet burner generates counterflow flames that are widely used to study chemical kinetics and molecular species transport under aerodynamic stretch. Using the opposed jet flames, partially premixed CH₄/air versus air flame structures were investigated [1]. Lean partially premixed methane and propane flame structures versus hot products have also been investigated [2, 3]. The present work tries to extend the previous work and stretch effects on the flame structure of the downstream interaction between hot products and lean C₃H₈/air mixtures are studied with Raman scattering and detailed transport, complex chemistry numerical simulations.

EXPERIMENTAL SYSTEM AND FLAMES EXAMINED

Measurement of major species and temperature are made along the centerline of an opposed jet burner using the laser Raman scattering technique. Four groups of flames classified by equivalence ratio are studied. Global stretch rate is defined by $\kappa=2V_o/L(1+\rho_f V_f^{1/2}/\rho_o V_o^{1/2})$. V and ρ are velocity and density of inlet gas streams respectively. Subscript o indicates oxidizer stream, subscript f indicates fuel stream. L is the separation distance between the two jets. In this work, honeycomb inserts replace the screens used previously [2, 3] and are placed flush with the tube exits to give very uniform jet exit velocity profiles. Group A includes three propane-air mixtures (which have a 0.75 equivalence ratios) versus a lean hydrogen-air mixture at stretch rates of 90, 140 and 252 s^{-1} respectively. Group B includes three propane-air mixtures which have a 0.66 equivalence ratio versus lean hydrogen-air mixture at stretch rates of 90, 140 and 252 s^{-1} . Group C includes two ultra lean sub-limit propane-air mixtures (equivalence ratio of 0.44 or 0.55) versus a lean hydrogen-air mixture at stretch rate 140 s^{-1} . Group D includes several stronger self-propagating flames. They are formed by propane-air mixtures which have equivalence ratios of 0.75, 0.86 or 1.25 versus air or hydrogen-air mixture at stretch rate 140 s^{-1} . All of lean hydrogen-air mixture has the same equivalence ratio: 0.28.

SIMULATION AND REACTION MECHANISMS

Numerical predictions are obtained from the "Oppdif" part of the CHEMKIN Collection [4]. Detailed chemical kinetic mechanisms and transport data are used for numerical predictions. A mechanism called the M5 propane mechanism by Haworth et al. [5], the Williams mechanism [6] and an Optimized mechanism of C1-C3 combustion

*Corresponding author: zhongxian.cheng@vanderbilt.edu

mechanism by Qin et al. [7] are used for the numerical simulation of propane-air flames.

RESULTS AND DISCUSSION

(1) Stretched propane-air flames with $\phi=0.75$

All flames shown in this subsection have the equivalence ratio ($\phi=0.75$). They are propane-air ($\phi=0.75$) versus hydrogen-air ($\phi=0.28$). It is known this kind of propane-air flame is above the lean flammability limit ($\phi=0.55$) [8]. The equivalence ratio for the two streams are fixed, the aerodynamic stretch rate varies from a relatively low 90 s^{-1} to near the extinction limit 252 s^{-1} .

Experimental measurements and numerical predictions of temperature and reactant concentrations are compared in Fig. 1 for the propane-air ($\phi=0.75$) mixture vs. hot products at a stretch rate of 140 s^{-1} . As seen from the experimental data, a premixed “positive flame speed” flame exists on the propane-air side of the stagnation plane. Numerical predictions are performed with three different chemical mechanisms (M5, Williams and Optimized mechanisms). The results shown in Fig. 1 are with the Williams mechanism. It is found that the premixed propane-air flame locates at 2.5 mm and the lean hydrogen-air flame locates at 9 mm downstream of the propane jet exit. The temperature profile implies that the two flames are far away each other. The predicted propane-air flame location is slightly off the actual location as seen in Fig. 1. Generally speaking, experimental data on propane-air flame side agree with numerical results. On the hydrogen-air flame side, there is very good agreement. Experimental data for temperature, oxygen concentration differs from the predicted results somewhat in the post flame zone. Carbon dioxide from the experiment is slightly lower than predicted. The water vapor from experimental data has very good agreement with predicted results. The comparison using different mechanisms is shown in Fig. 2. From Fig. 2, it is seen that the predictions using the M5 and Optimized mechanisms do not match the data as well. The most obvious deviation is the propane-air flame location. This may be caused by different flame propagating speeds for the various chemical kinetic mechanisms. In contrast, measured and calculated flame temperature and species concentration agree very well on the hydrogen-air flame side. The chemical mechanism is relatively simple and well known for hydrogen-air. From Fig. 2, it is indicated that the Williams mechanism predicts a higher laminar flame speed for both hydrogen-air and propane-air flames. The results from the M5 mechanism and the Optimized mechanism are almost identical at this stretch rate.

Keeping everything unchanged except stretch rate, the flame structure near extinction condition ($\kappa=252 \text{ s}^{-1}$) is given Fig. 3. This is a very weak diffusion controlled flame. The peak temperature is around 1400 K. The experimental data agree very well with predicted results from the Optimized mechanism, but deviates from the prediction by

the M5 or the Williams mechanisms. The numerical results with Williams mechanism indicate a strong premixed flame for this situation (temperature is about 1800 K). On the other hand, results from the M5 mechanism indicate extinction occurred. At the high stretch rate, the flame structure is sensitive to different chemical kinetic mechanisms.

The thermal diffusivity coefficient of lean propane-air mixture is $0.208 \text{ cm}^2/\text{s}$ and mass diffusivity (propane in air) are $0.114 \text{ cm}^2/\text{s}$. Thus the Lewis number of the deficient reactant which is the ratio of thermal diffusivity to mass diffusivity is 1.82 and much greater than unity. Therefore the lean propane-air mixture has unbalanced preferential diffusion. According to Law [9] and Sung et al. [10], the combination of stretch rate and Lewis number effect will cause for flame temperature to decrease with stretch rate for $L_e > 1$. The flame structure for $\kappa=90 \text{ s}^{-1}$ is shown in Fig. 4. The temperature is higher when stretch rate drops from 140 s^{-1} to 90 s^{-1} .

(2) Stretched propane-air flames with $\phi=0.66$

All flames shown in this subsection have the same equivalence ratio: propane-air ($\phi=0.66$) vs. hydrogen-air ($\phi=0.28$). Again, the aerodynamic stretch rate varies from 90 s^{-1} to near extinction (252 s^{-1}). Compared to Group A, they are slightly leaner mixtures. At $\kappa=90 \text{ s}^{-1}$, the flame structure (not shown) is similar to the structure for $\phi=0.75$ (Fig. 4). The only difference is the flame moves towards the stagnation plane. This is because the flame speed decreases and the stretch rate is unchanged.

When increasing the stretch rate to $\kappa=140 \text{ s}^{-1}$, the lean premixed propane-air mixture diffuses across the stagnation plane to form a weak diffusion flame. The stagnation plane is penetrable. The flame structure is shown in Fig. 5. The numerical simulation comes from the Optimized mechanism and the M5 mechanism. Comparing experimental data with predictions indicates temperature and most of the species concentrations agree well except carbon-dioxide. The experimental carbon-dioxide data agree with predictions from the Optimized mechanism better than that from the M5 mechanism. These results are consistent with previous work by Wehrmeyer et al. [2] that shows the M5 mechanism gives a carbon dioxide prediction that is one order of magnitude lower than the experimental data. When this flame is modeled by the Williams mechanism, the flame structure is different and it is shown in Fig. 6. Obviously the predictions with the Williams mechanism are far away from the experimental data.

Figure 7 shows the flame structure for a stretch rate of 252 s^{-1} using the Williams and Optimized mechanisms. The M5 mechanism gives extinction. The flame itself is very similar to $\kappa=140 \text{ s}^{-1}$, except the reaction zone is narrower. Usually for the diffusion flame, the flame thickness inversely scales with $\kappa^{1/2}$. Here it is not a pure diffusion flame but is composed of a negative flame speed

methane-air diffusion flame and a lean premixed hydrogen-air flame. But the trend is still true for this case, that is, the flame reaction zone is becoming narrower when increasing stretch rate. Similarly, incomplete reaction caused by higher stretch rate eventually leads to extinction even though hot products in downstream can extend this extinction up to much higher level.

(3) Stretched sublimit propane-air flames

The lean limit for a propane-air mixture is 5% (by volume) or $\phi=0.55$. Based on the definition of flammability limit, the mixture will be impossible to burn at any condition if it is under the lean limit. But, Ju et al. [11, 12] numerically studied the sublimit combustion at very low stretch rate and found that sublimit flames can exist. Particularly for premixed flames with deficient Lewis numbers less than one. Here our planar flame experiment shows that the extinction limit is dependent on external conditions such as preferential diffusion, stretch rate and support of hot products. For the propane-air flame, the mixture lean limit can be very low if the mixture interacts with hot products from the hydrogen-air flame, even though the flame is very weak. Hot products commonly exist in turbulent combustion and can support the burning of very lean mixtures.

Figure 8 shows the sublimit flame structure of C_3H_8 -Air mixture ($\phi=0.44$) versus H_2 -Air ($\phi=0.28$) mixture ($\kappa=140\text{ s}^{-1}$). This is a very weak negative flame speed flame. The flame temperature drops to 1300 K, just above the minimum ignition temperature. Predictions based on the Williams mechanism give good agreement with experiment data for temperature and most reactants except carbon-dioxide. The measured carbon dioxide is 50% higher than predicted. Unlike the negative flame speed flames shown previously, the Williams mechanism works well for the ultra weak flame, the M5 mechanism predicts a slightly weaker flame, but the Optimized mechanism gives an extinction prediction. Fig. 9 shows another lean limit flame structure: C_3H_8 -Air mixture ($\phi=0.55$) versus H_2 -Air ($\phi=0.28$) mixture ($\kappa=140\text{ s}^{-1}$). The flame temperature is still around 1300 K. There is a good agreement for temperature and species including carbon dioxide. The comparisons of three mechanisms are given in Fig. 10. This mixture is very near the lean flammability limit and the three mechanisms have similar predictions even though there are slight differences in carbon dioxide profiles.

(4) Stretched near-stoichiometric flames

In order to further demonstrate the Lewis number effect on premixed propane-air flame structure, relatively stronger flames are studied. One of those flame structures is shown in Fig. 11. It is a premixed propane-air mixture ($\phi=0.86$) versus air at stretch rate 140 s^{-1} . The measured peak temperature is close to 2200 K and slightly higher than

predicted. The trend for species is similar to that shown in Fig. 1.

CONCLUSIONS

Stretched laminar flame structures for a wide range propane-air mixtures versus hot products are investigated by laser-based diagnostics and numerical simulation. The stretch effect and influence of equivalence ratio on flame structure are studied in detail.

For self-propagating flames, the measured water vapor agrees very well with numerical predictions. Measured temperature, oxygen, carbon dioxide slightly deviate from the predicted results. Premixed flame locations are different with various kinetic mechanisms. The measured flame location is close to predicted with the Williams mechanism.

For diffusion controlled negative flame speed flames above the lean limit ($\phi>0.55$), most species concentration and temperature have very good agreement between experimental data and predicted results except carbon dioxide. The predicted carbon dioxide concentration with the M5 mechanism is much lower than experimental data, while the Optimized propane mechanism gives good predicted results compared to experimental data. The prediction with Williams mechanism gives a self-propagating flame structure at $\kappa=140\text{ s}^{-1}$ while the M5 mechanism and the Optimized mechanism give diffusion controlled negative flame speed flame structure.

For sub-limit flame structure ($\phi<0.55$) predictions with Williams mechanism is closest to experimental data even though there is some deviation for the carbon dioxide profile. The Optimized mechanism predicts an extinction while other two mechanism give good results. At the lean limit ($\phi=0.55$), All three mechanisms give different predictions for carbon dioxide.

ACKNOWLEDGEMENTS

The authors would like to acknowledge the U.S. Department of Energy's Office of Basic Energy Sciences who have supported this work through a Partnerships for Academic-Industrial Research (PAIR) grant (No. DE-FG02-98ER14915, with Dr. Alan H. Laufer as the technical monitor).

REFERENCES

1. Tanoff, M. A., Smooke, M. D., Osborne, R. J., Brown, T. M., Pitz, R. W. (1996), "The Sensitive Structure of Partially Premixed Methane-Air vs. Air Counterflow Flames," *Proceedings of the Combustion Institute* **26**, pp. 1121-1128.
2. Wehrmeyer, J. A., Cheng, Z., Mosbacher, D. M., Pitz, R. W., Osborne, R. J. (2002), "Opposed Jet Flames of Lean or Rich Premixed Propane-Air Reactants versus Hot Products," *Combustion and Flame* **128**, pp. 232-241.

3. Cheng, Z., Wehrmeyer, J. A., Pitz, R. W. (2002), "Opposed Jet Flames of Lean Premixed Methane-Air Reactants vs. Hot Products," Paper AIAA 2002-4021, 38th AIAA Joint Propulsion Conference, Indianapolis, IN, July 7-10.
4. Kee, R. J., Rupley, F., Miller, J., Coltrin, M., Grcar, J., Meeks, E., Moffat, H., Lutz, A., Dixon-Lewis, G., Smooke, M., Warnatz, J., Evans, G., Larson, R., Mitchell, R., Petzold, L., Reynolds, L., Caracotsios, M., Stewart, W., Glarborg, P. (1999), *User Manual, CHEMKIN Collection III*.
5. Haworth, D. C., Blint, R. J., Cuenot, B., Poinot, T. J. (2000), "Numerical Simulation of Turbulent Propane-Air Combustion with Nonhomogeneous Reactants," *Combustion and Flame* **121**, pp. 395-417.
6. <http://maeweb.ucsd.edu/~combustion/cermec/>
7. Qin, Z., Lissianski, V., Yang, H., Gardiner, W., Davis, S., Wang, H. (2000), "Combustion Chemistry of Propane: A Case Study of Detailed Reaction Mechanism Optimization," *Proceedings of the Combustion Institute* **28**, pp. 1663-1669.
8. Glassman, I., *Combustion*, Third edition, Academic Press, San Diego, CA, 1996.
9. Law, C. K. (1988), "Dynamics of Stretch Flames," *Proceedings of the Combustion Institute* **22**, pp. 1381-1402.
10. Sung, C. J., Liu, J. B., and Law, C. K. (1996), "On the Scalar Structure of Nonequidifusive Premixed Flames in Counterflow," *Combustion and Flame* **106**, pp. 168-183.
11. Ju, Y., Matsumi, H., Takita, K., and Masuya, G., (1999), "Combined Effects of Radiation, Flame Curvature, and Stretch on the Extinction and Bifurcations of Cylindrical CH₄/Air Premixed Flame," *Combustion and Flame* **116**, pp. 580-592.
12. Ju, Y., Guo, H., Maruta, K., Niioka, T. (1998), "Flame Bifurcations and Flammable Regions of Radiative Counterflow Premixed Flames with General Lewis Numbers," *Combustion and Flame* **113**, pp. 603-614.

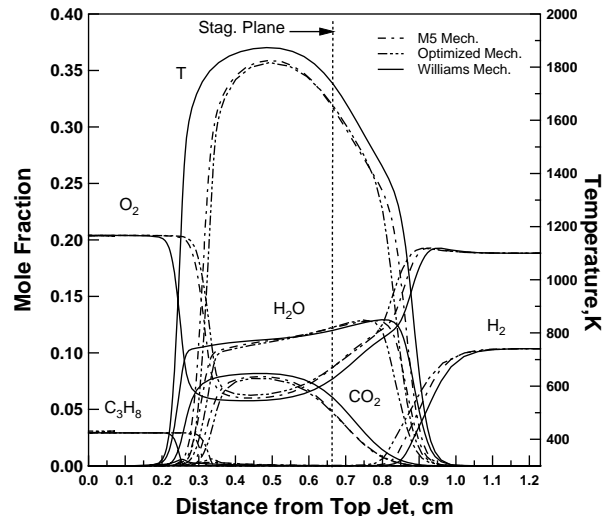
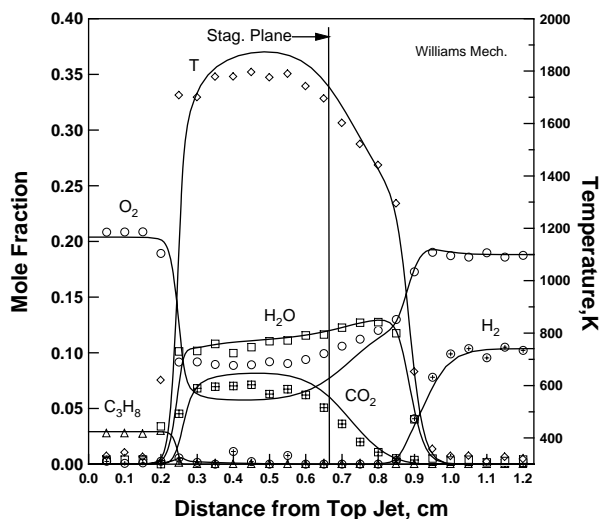


Fig. 2. The comparison of numerically-predicted species and temperature profiles with three different mechanisms for a flame: C₃H₈-air ($\phi=0.75$) vs. H₂-air ($\phi=0.28$), $\kappa=140 \text{ s}^{-1}$.

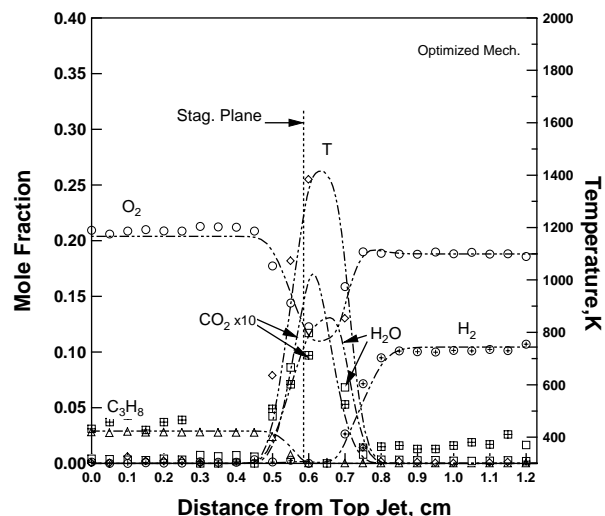


Fig. 3. Experimental and numerical-predicted species and temperature profiles for a flame: C₃H₈-air ($\phi=0.75$) vs. H₂-air ($\phi=0.28$), $\kappa=252 \text{ s}^{-1}$. Numerical simulation using Optimized mechanism.

Fig. 1. Experimental and numerical-predicted species and temperature profiles for a flame: C₃H₈-air ($\phi=0.75$) vs. H₂-air ($\phi=0.28$), $\kappa=140 \text{ s}^{-1}$. Numerical simulation using Williams mechanism

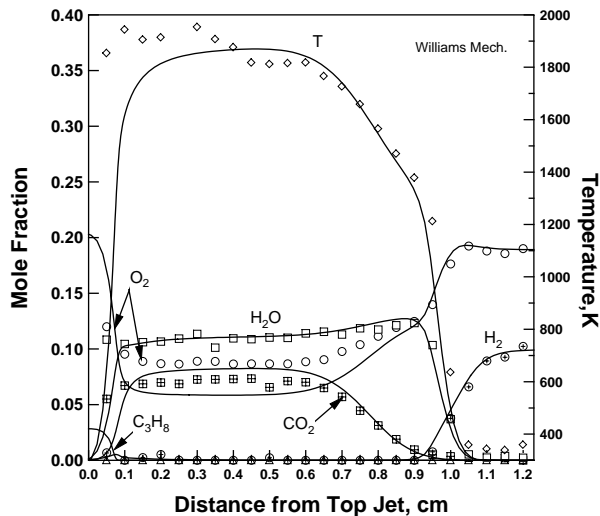


Fig. 4. Experimental and numerical-predicted species and temperature profiles for a flame: C_3H_8 -air ($\phi=0.75$) vs. H_2 -air ($\phi=0.28$), $\kappa=90 \text{ s}^{-1}$. Numerical simulation using Williams mechanism.

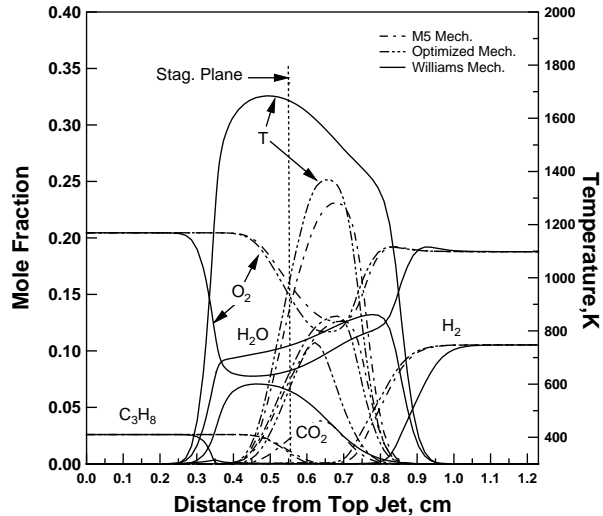


Fig. 6. The comparison of numerically-predicted species and temperature profiles with three different mechanisms for a flame: C_3H_8 -air ($\phi=0.66$) vs. H_2 -air ($\phi=0.28$), $\kappa=140 \text{ s}^{-1}$.

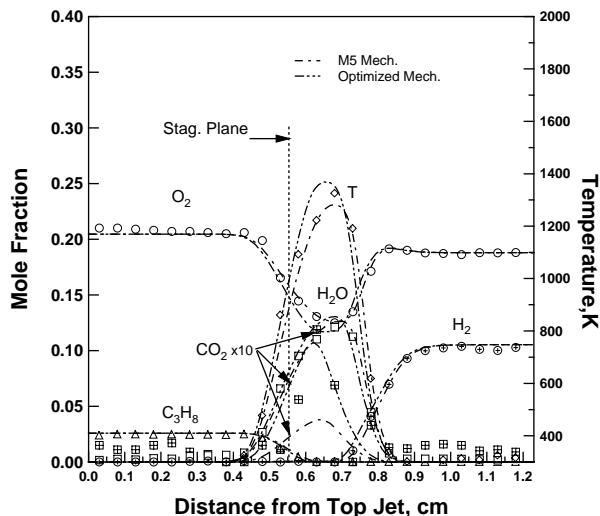


Fig. 5. Experimental and numerical-predicted species and temperature profiles for a flame: C_3H_8 -air ($\phi=0.66$) vs. H_2 -air ($\phi=0.28$), $\kappa=140 \text{ s}^{-1}$. Numerical simulation using M5 and Optimized mechanisms.

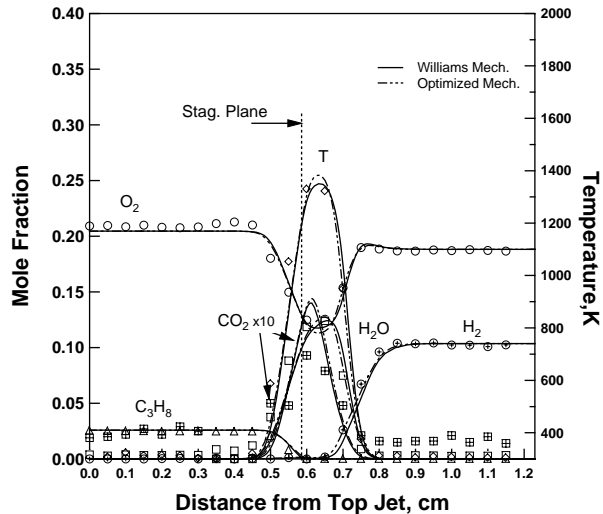


Fig. 7. Experimental and numerical-predicted species and temperature profiles for a flame: C_3H_8 -air ($\phi=0.66$) vs. H_2 -air ($\phi=0.28$), $\kappa=252 \text{ s}^{-1}$. Numerical simulation using Williams and Optimized mechanisms.

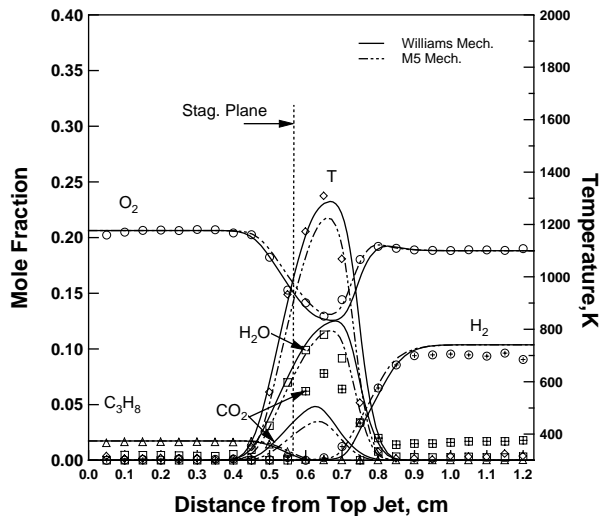


Fig. 8. Experimental and numerical-predicted species and temperature profiles for a flame: C_3H_8 -air ($\phi=0.44$) vs. H_2 -air ($\phi=0.28$), $\kappa=140\text{ s}^{-1}$. Numerical simulation using M5 and Williams mechanisms.

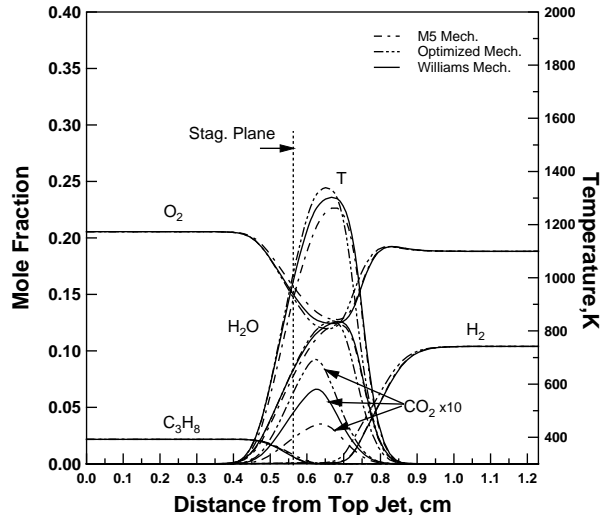


Fig. 10. The comparison of numerically-predicted species and temperature profiles with three different mechanisms for a flame: C_3H_8 -air ($\phi=0.55$) vs. H_2 -air ($\phi=0.28$), $\kappa=140\text{ s}^{-1}$.

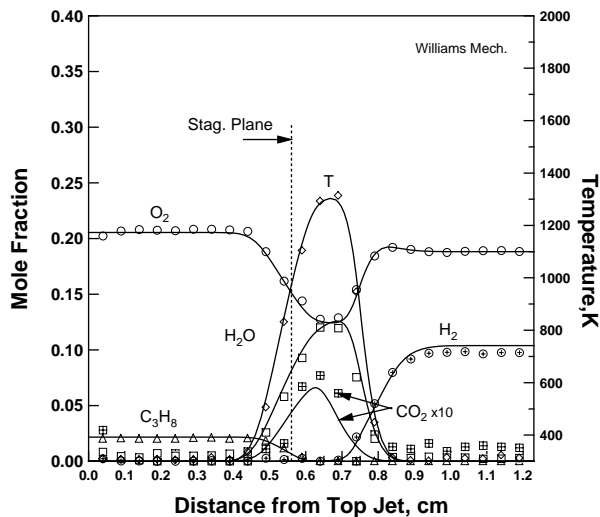


Fig. 9. Experimental and numerical-predicted species and temperature profiles for a flame: C_3H_8 -air ($\phi=0.55$) vs. H_2 -air ($\phi=0.28$), $\kappa=140\text{ s}^{-1}$. Numerical simulation using Williams mechanism.

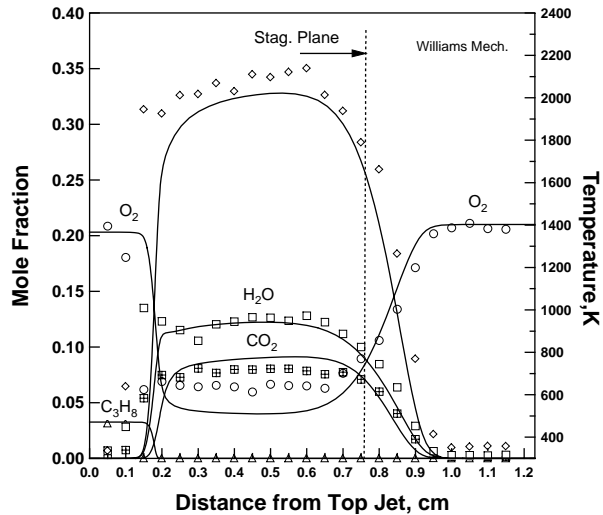


Fig. 11. Experimental and numerical-predicted species and temperature profiles for a flame: C_3H_8 -air ($\phi=0.86$) vs. air, $\kappa=140\text{ s}^{-1}$. Numerical simulation using mechanisms.